

Supplementary Information

Localised degradation within sulfide-based all-solid-state electrodes visualised by Raman mapping

Jungwoo Lim^{a,b}, Yundong Zhou^{a,b,c}, Rory H. Powell^{a,b}, Tugce Ates^{d,e}, Stefano Passerini^{d,e,f} and Laurence J. Hardwick^{a,b,*}

^a Stephenson Institute for Renewable Energy, Department of Chemistry, University of Liverpool, L69 7ZF Liverpool, United Kingdom

^b The Faraday Institution, Harwell Campus, Didcot, OX11 0RA, United Kingdom

^c Present Address: National Physical Laboratory, Hampton Rd, Teddington TW11 0LW, United Kingdom

^d Helmholtz Institute Ulm (HIU), Helmholtzstrasse 11, 89081 Ulm, Germany

^e Karlsruhe Institute of Technology (KIT), P.O. Box 3640, 76021 Karlsruhe, Germany

^f Chemistry Department, Sapienza University of Rome, Piazzale A. Moro 5, 00185 Rome, Italy

Corresponding author: hardwick@liverpool.ac.uk

1. Experimental

1.1 Materials

$\text{LiNi}_{0.6}\text{Mn}_{0.2}\text{Co}_{0.2}\text{O}_2$, $\beta\text{-Li}_3\text{PS}_4$, $\text{Li}_6\text{PS}_5\text{Cl}$ (Ampcera™) and $\text{Li}_{10}\text{GeP}_2\text{S}_{12}$ were all received from MSE supplies and opened in an argon-filled glovebox (O_2 , H_2O level < 0.1 ppm). Vapour grown carbon fibre (VGCF, Sigma Aldrich, 98% carbon-basis) was used as the conductive carbon additive. Polyisobutene (OPPANOL®, BASF) was used as a binder and was dissolved in toluene (Anhydrous, 99.8%, Sigma Aldrich) (5 wt%) during slurry preparation. Lithium bis(trifluoromethanesulfonyl)imide (LiTFSI, 99.9%, Solvionic) and polyethylene oxide (PEO, Sigma Aldrich) were used as an interlayer between the solid electrolyte and lithium metal.

1.2 Solid-state cell preparation

Within an argon containing glovebox, $\text{LiNi}_{0.6}\text{Mn}_{0.2}\text{Co}_{0.2}\text{O}_2$ was mixed with either $\beta\text{-Li}_3\text{PS}_4$, $\text{Li}_6\text{PS}_5\text{Cl}$ or $\text{Li}_{10}\text{GeP}_2\text{S}_{12}$, VGCF, OPPANOL® (49:37:8:6 wt%) and ground together for 30 minutes in a mortar and pestle. Toluene was then added to the mixed powder. The mixture was then tape-cast onto Al foil (thickness: 20 μm) and dried under vacuum at room temperature overnight. For solid-state cells made with $\beta\text{-Li}_3\text{PS}_4$, the $\beta\text{-Li}_3\text{PS}_4$ in the toluene solvent was cast onto Al foil and dried in vacuum at room temperature and punched (diameter: 5 mm). After punching, Al foil was removed, and the free-standing solid electrolyte layer was pressed together with the positive electrode at 3.5 tonne for 5 mins.

For $\text{Li}_6\text{PS}_5\text{Cl}$, and $\text{Li}_{10}\text{GeP}_2\text{S}_{12}$ containing cells, 25 mg of respective solid electrolyte powder was spread onto the punched 5-mm electrode and pressed at 3.5 tonne for 5 minutes. For Li_3PS_4 cells, an additional 10 wt% LiTFSI-containing PEO layer (thickness: ca. 100 μm) was first put on the Li metal as an additional protective barrier. The solid-state cells against Li metal were cycled at a C-rate of C/20 at 60 °C for $\beta\text{-Li}_3\text{PS}_4$, and 25 °C for $\text{Li}_6\text{PS}_5\text{Cl}$, and $\text{Li}_{10}\text{GeP}_2\text{S}_{12}$ in two-electrode Swagelok cells cycled in Maccor (Maccor 4000 series) from 3 ~ 4.2 V vs. Li/Li⁺.

For the cell measurement with liquid electrolyte (**Figure S1**), the electrode was cast with $\text{LiNi}_{0.6}\text{Mn}_{0.2}\text{Co}_{0.2}\text{O}_2$, carbon black (Super P, Timcal) and polyvinylidene fluoride (Kynar-Flex 2801) binder mixed in N-methyl-2-pyrrolidone (anhydrous, Aldrich) in the ratio 80:10:10. 1 M of LiPF_6 dissolved in carbonate based electrolyte (ethylene carbonate: dimethyl carbonate = 1: 1, v/v) was used for electrolyte.

1.3 Characterisation

All the samples are sealed by hermetically sealed optical cells and measured through a thin quartz window (ca. 0.2 mm thick) under inert argon atmosphere. *Ex situ* Raman analysis on positive electrodes were performed with Raman microscope (Renishaw, in via Reflex coupled with an inverted Leica microscope), with a 633 nm laser as excitation source (43 μ W at electrode surface), focused on to the sample using a x50 objective (Olympus). Collection mode was 10 seconds with 3 accumulations. For Raman contour mapping, spectra were collected at 400 points within a 20 \times 20 μ m area upon the solid-state positive electrode surface. 20 μ m \times 20 μ m was selected as it is large enough to capture part or whole of at least one particle $\text{LiNi}_{0.6}\text{Mn}_{0.2}\text{Co}_{0.2}\text{O}_2$ where typical diameter is lower than 10 μ m (**Figure S2**). The area of each component was then integrated using WiRE software. For each component, the value for the 400 points were used to plot contour mapping images. To exclude any laser heating effects leading to, in particular the decomposition of the electrolytes, during electrode mapping each component (3 solid electrolyte, $\text{LiNi}_{0.6}\text{Mn}_{0.2}\text{Co}_{0.2}\text{O}_2$, VGCF) had their Raman spectrum collected with increasing laser power (43, 215, 430 μ W and 2.15 mW). The exposure time was 10s for 3 solid electrolytes, 40s for $\text{LiNi}_{0.6}\text{Mn}_{0.2}\text{Co}_{0.2}\text{O}_2$ and 80s for VGCF. No change in the Raman spectra in any of the components was observed as laser power was increased from 43 μ W to fifty times more intense (2.15 mW). Scanning electron microscopy (SEM) measurements were conducted using a JEOL JSM-6610 system after Pt deposition.

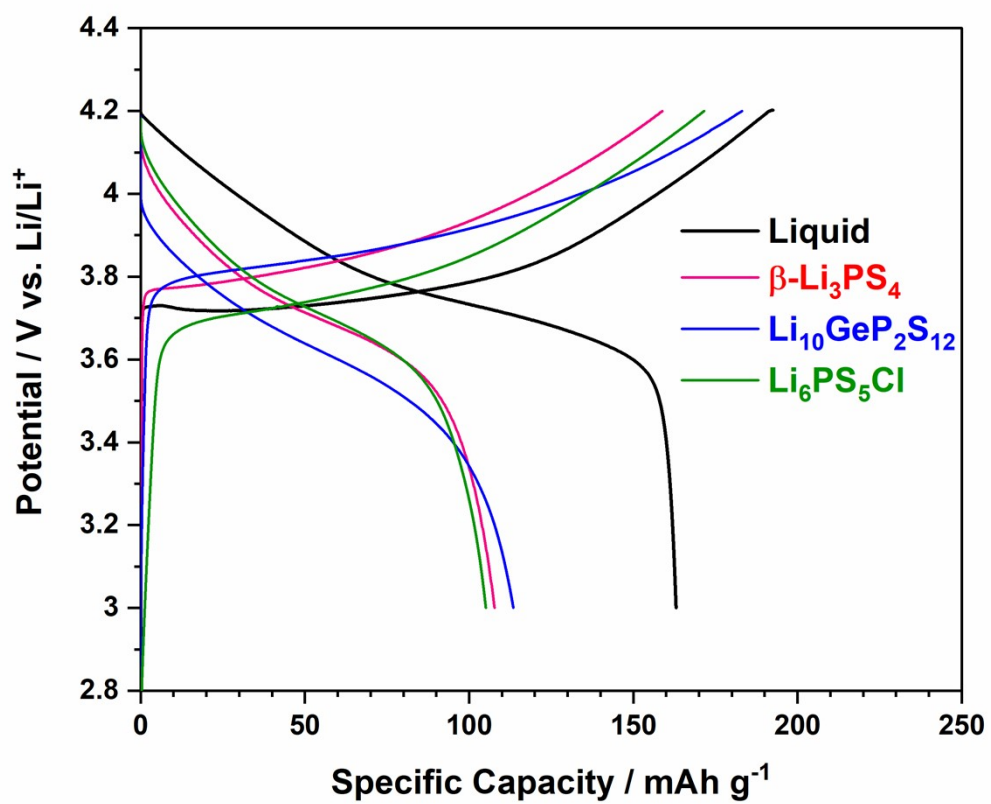


Figure S1. Voltage profile of $\text{LiNi}_{0.6}\text{Mn}_{0.2}\text{Co}_{0.2}\text{O}_2$ cycled at 3 - 4.2 V vs. Li/Li^+ with liquid electrolyte (1 M LiPF_6 in EC: DMC = 1:1 v/v solution) and the three-sulfide based solid electrolytes: $\beta\text{-Li}_3\text{PS}_4$, $\text{Li}_{10}\text{GeP}_2\text{S}_{12}$ and $\text{Li}_6\text{PS}_5\text{Cl}$.

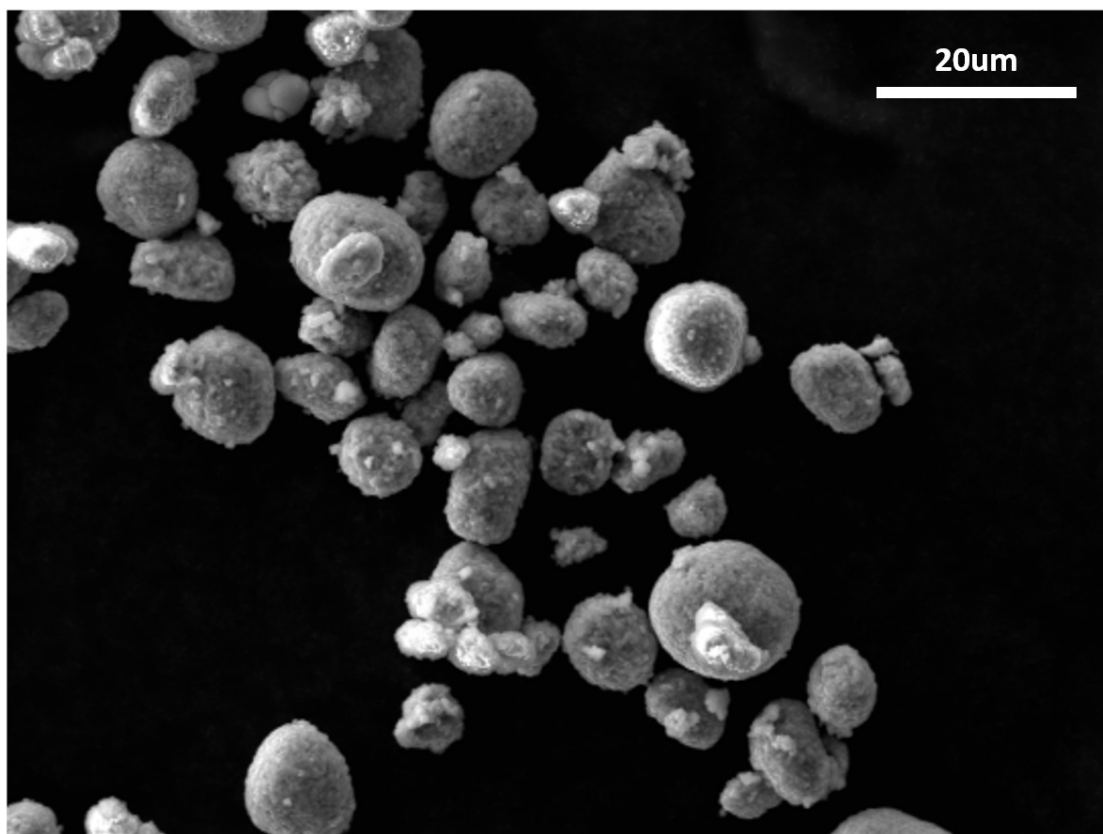


Figure S2. SEM image of LiNi_{0.6}Mn_{0.2}Co_{0.2}O₂ powder, primary particle sizes in the range of 5-15 micron.

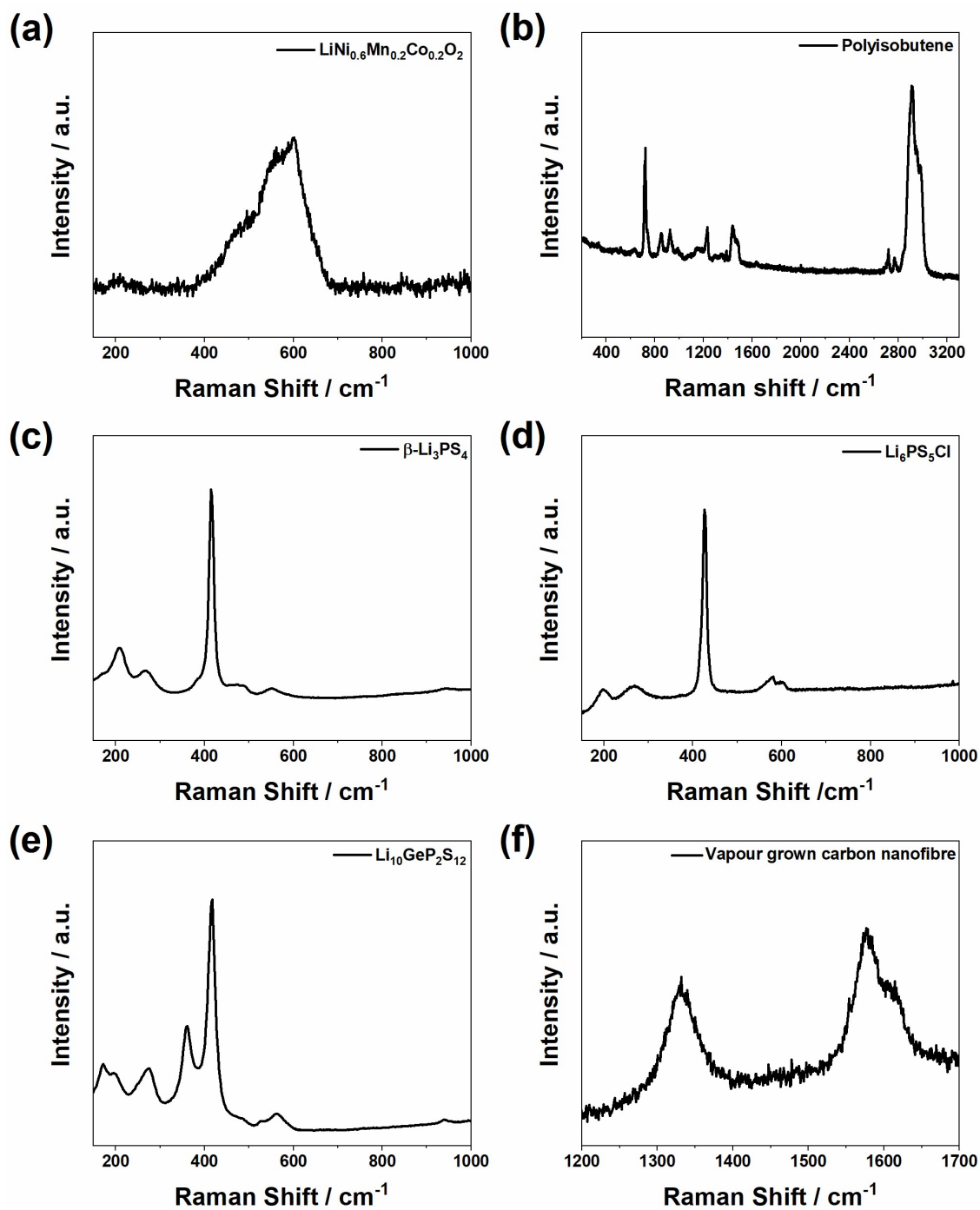


Figure S3. Raman spectra of pristine materials (a) $\text{LiNi}_{0.6}\text{Mn}_{0.2}\text{Co}_{0.2}\text{O}_2$, (b) polyisobutene (Oppanol[®]), (c) $\beta\text{-Li}_3\text{PS}_4$, (d) $\text{Li}_6\text{PS}_5\text{Cl}$, (e) $\text{Li}_{10}\text{GeP}_2\text{S}_{12}$ and (f) Vapour grown carbon nanofibre.

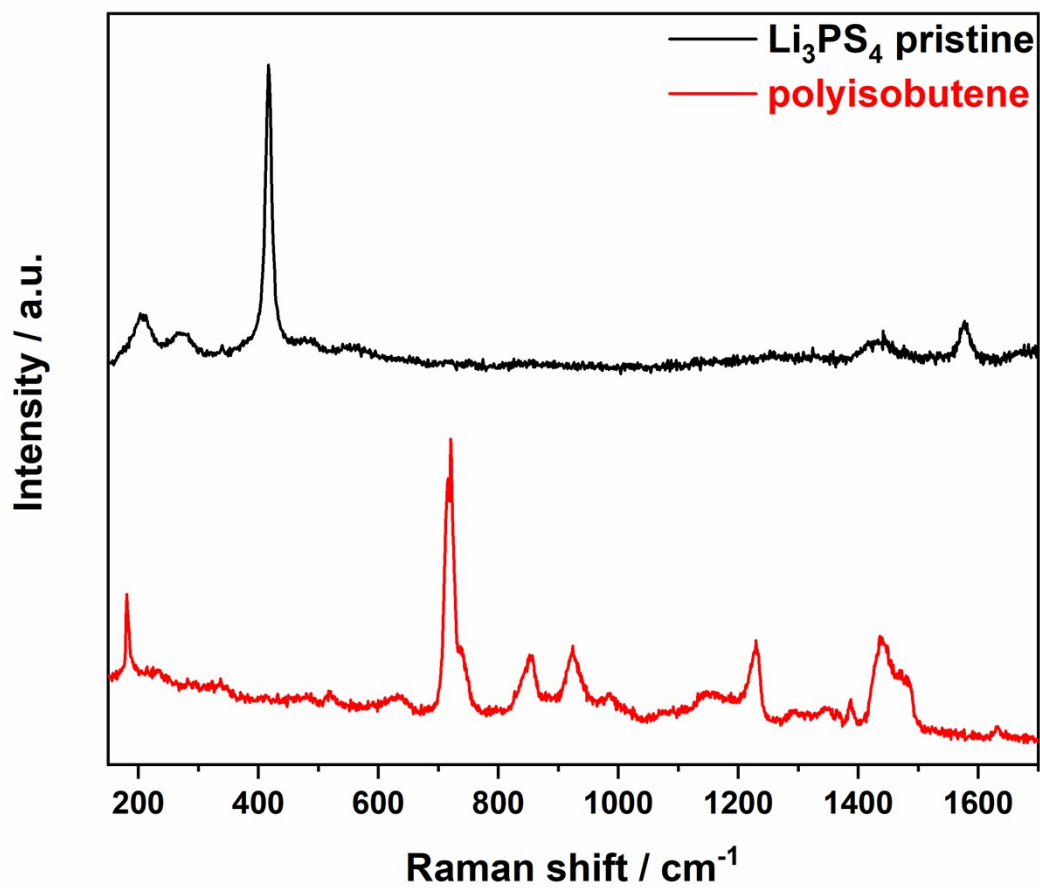


Figure S4. Raman spectra of polyisobutene (Oppanol) and β -Li₃PS₄ based LiNi_{0.6}Mn_{0.2}Co_{0.2}O₂ pristine electrode also plotted within Figure 2(a).

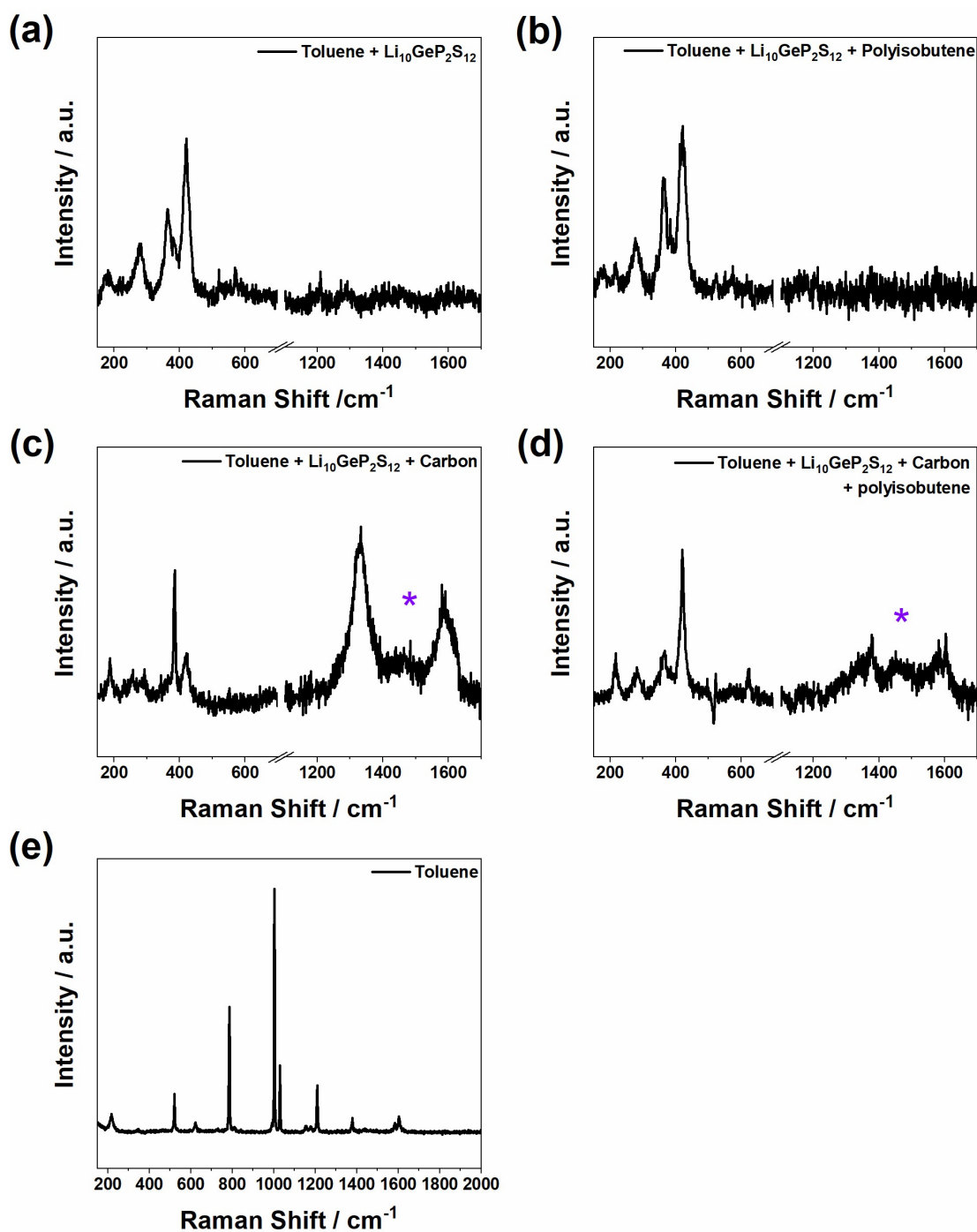


Figure S5. Raman spectra collected from stoichiometric slurry mixture. (a) Toluene + $\text{Li}_{10}\text{GeP}_2\text{S}_{12}$, (b) Toluene + $\text{Li}_{10}\text{GeP}_2\text{S}_{12}$ + polyisobutene, (c) Toluene + $\text{Li}_{10}\text{GeP}_2\text{S}_{12}$ + carbon (VGCF) + polyisobutene, (d) Toluene + $\text{Li}_{10}\text{GeP}_2\text{S}_{12}$ + Carbon and (e) Toluene (solvent only). * Indicates decomposition product at 1430 cm^{-1} assigned as $\delta(\text{CH}_3)\text{-S}$.

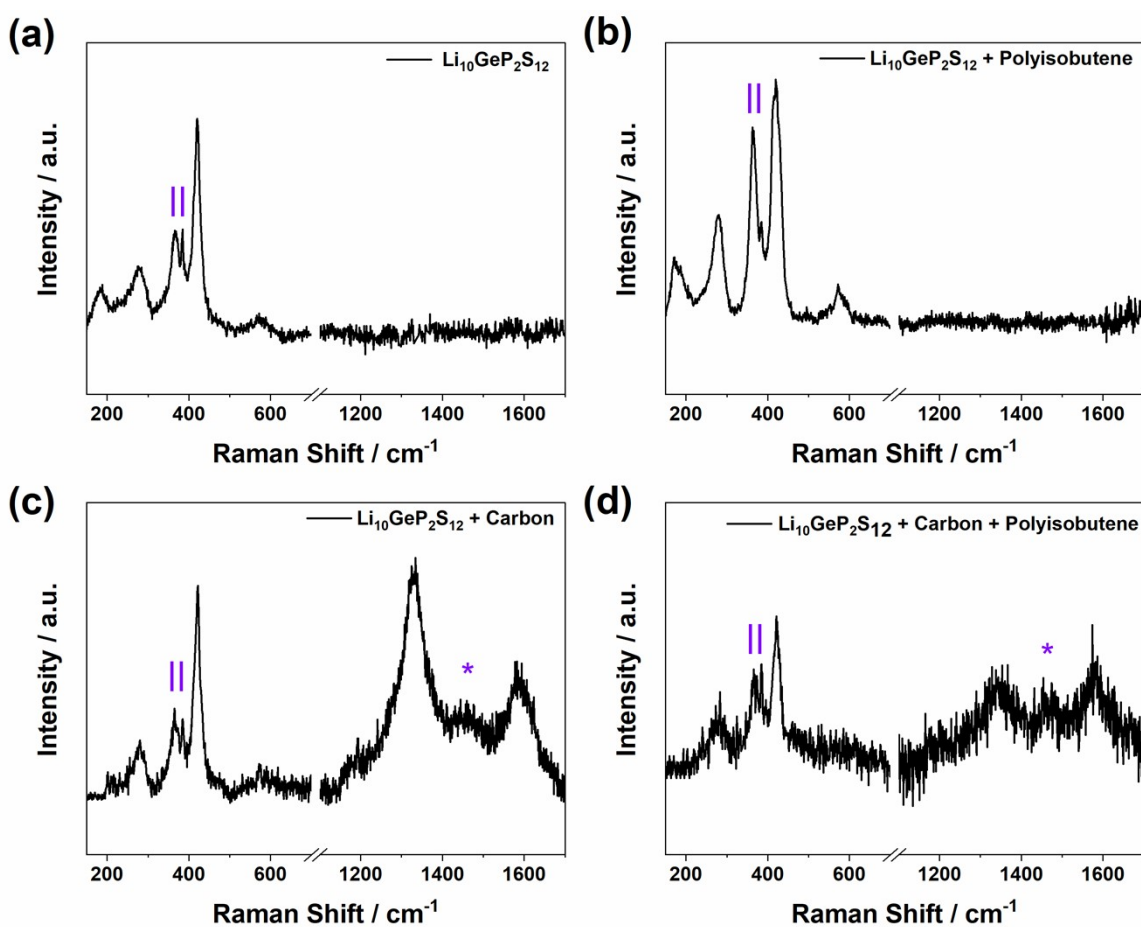


Figure S6. Raman spectra collected from stoichiometric slurry mixture after drying at vacuum. (a) $\text{Li}_{10}\text{GeP}_2\text{S}_{12}$, (b) $\text{Li}_{10}\text{GeP}_2\text{S}_{12}$ + polyisobutene, (c) $\text{Li}_{10}\text{GeP}_2\text{S}_{12}$ + carbon (VGCF) and (d) $\text{Li}_{10}\text{GeP}_2\text{S}_{12}$ + carbon + polyisobutene. *Indicates chemical decomposition product at 1430 cm⁻¹ (assigned as $\delta(\text{CH}_3)\text{-S}$) and purple bar indicates $(\text{GeS}_4)^{3-}$ framework of $\text{Li}_{10}\text{GeP}_2\text{S}_{12}$ and decomposition product GeS_2 .

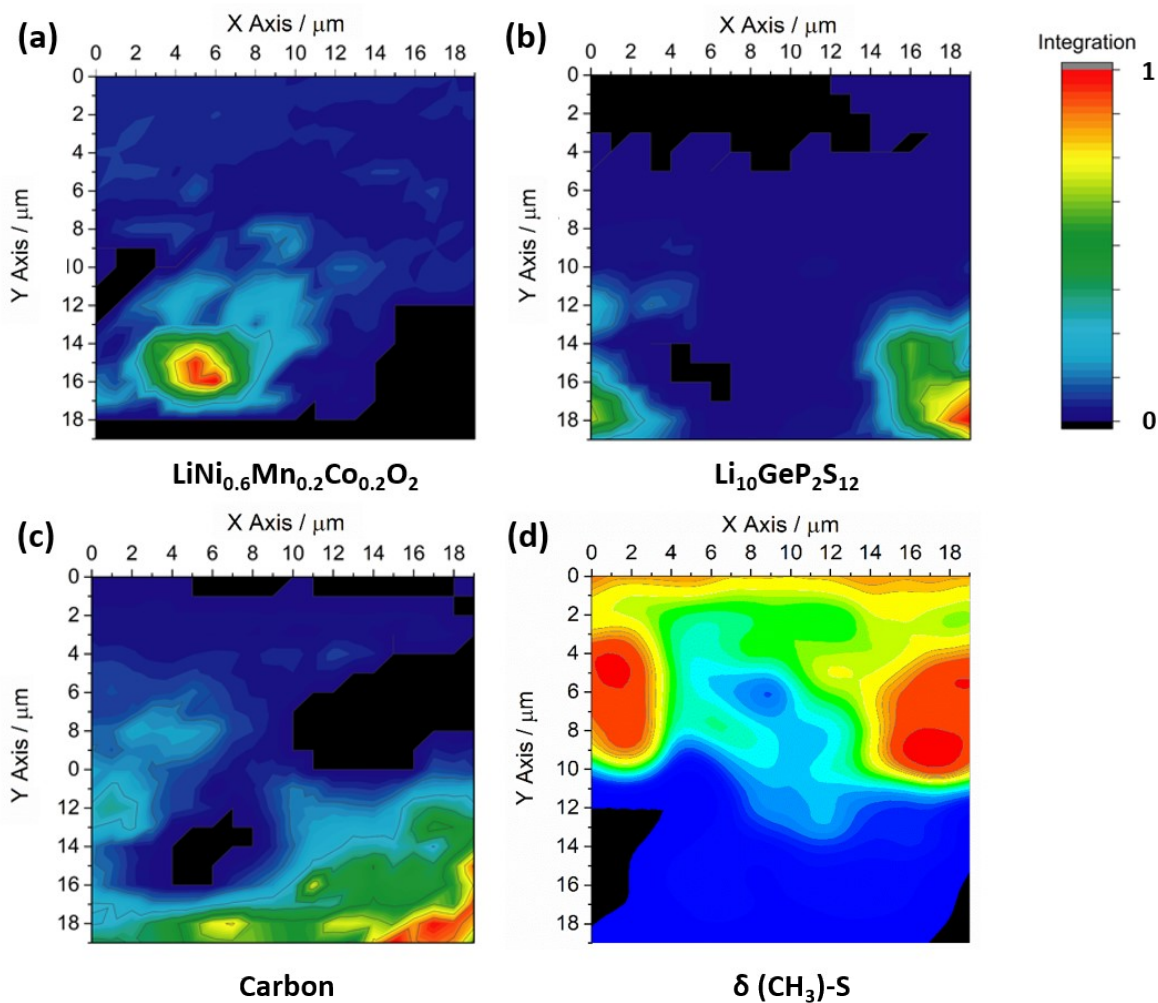


Figure S7. Raman mapping image of pristine $\text{Li}_{10}\text{GeP}_2\text{S}_{12}$ containing composite electrode, (a) bands of $\text{LiNi}_{0.6}\text{Mn}_{0.2}\text{Co}_{0.2}\text{O}_2$, (b) band of $\text{Li}_{10}\text{GeP}_2\text{S}_{12}$, (c) band of carbon additive (VGCF) and (d) $\delta(\text{CH}_3)\text{-S}$. Red contours represent presence of intense bands, blue contour trace presence and black, band not detected.

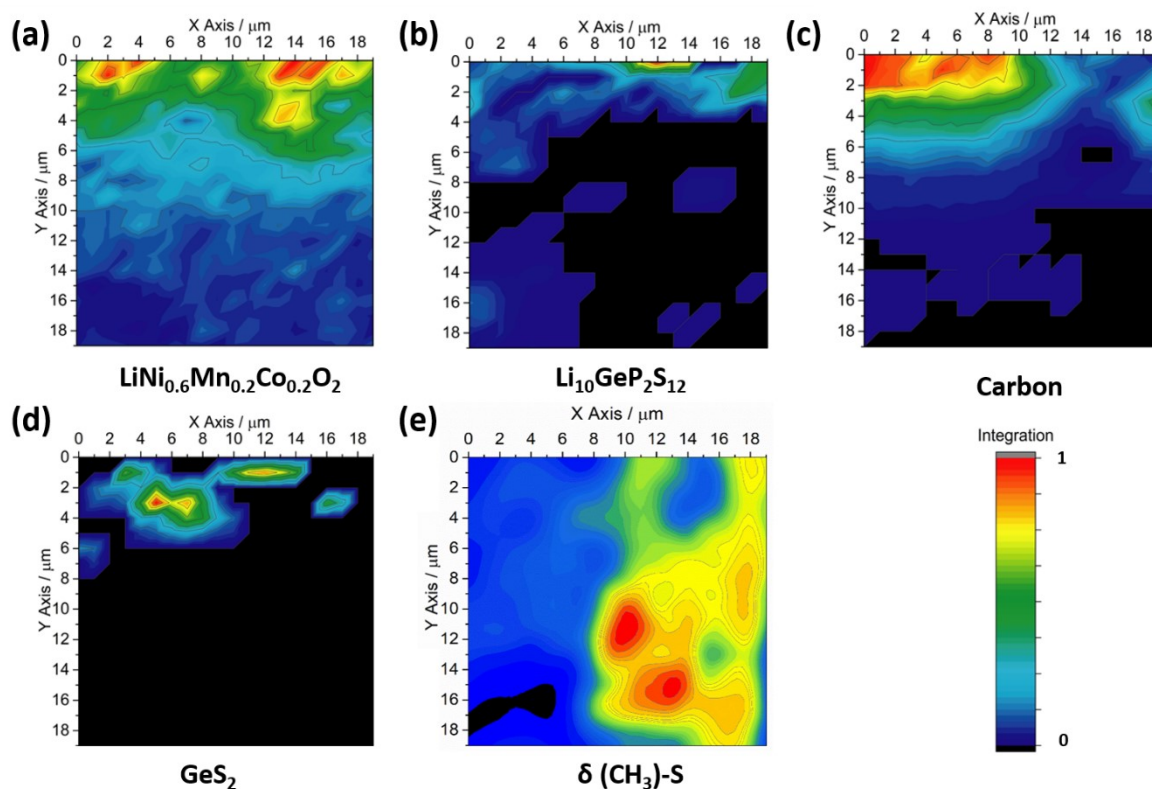


Figure S8. GeS_2 observed on $\text{LiNi}_{0.6}\text{Mn}_{0.2}\text{Co}_{0.2}\text{O}_2$ at location where there was significant amount of $\text{Li}_{10}\text{GeP}_2\text{S}_{12}$ and carbon additive present. Raman mapping images of $\text{Li}_{10}\text{GeP}_2\text{S}_{12}$ containing composite electrode after electrochemical cycling (a) $\text{LiNi}_{0.6}\text{Mn}_{0.2}\text{Co}_{0.2}\text{O}_2$, (b) $\text{Li}_{10}\text{GeP}_2\text{S}_{12}$, (c) carbon additive (VGCF), (d) band from decomposition product GeS_2 and (e) $\delta(\text{CH}_3)\text{-S}$.

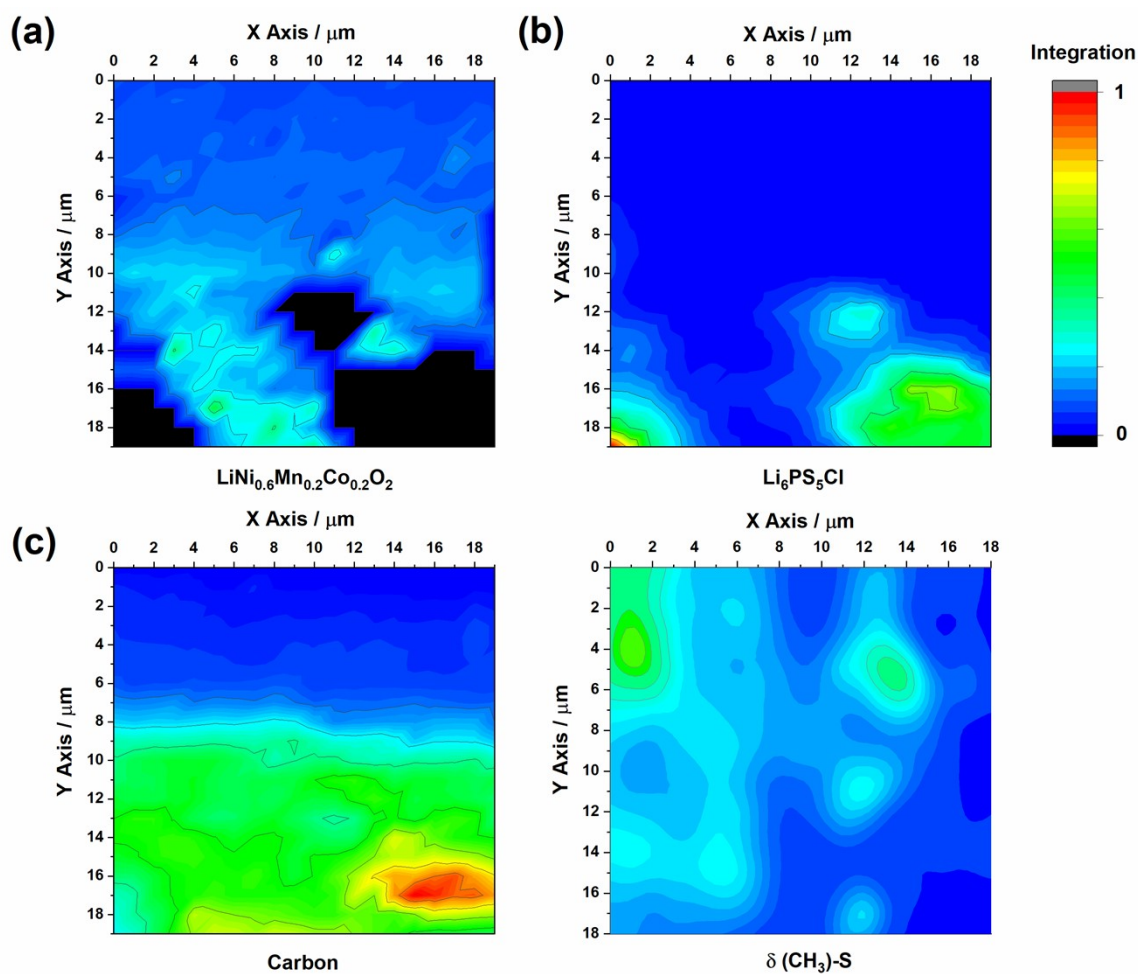


Figure S9. Raman mapping images of pristine $\text{Li}_6\text{PS}_5\text{Cl}$ containing composite electrode, (a) $\text{LiNi}_{0.6}\text{Mn}_{0.2}\text{Co}_{0.2}\text{O}_2$, (b) $\text{Li}_6\text{PS}_5\text{Cl}$ and (c) carbon additive (VGCF) and (d) $\delta(\text{CH}_3)\text{-S}$.

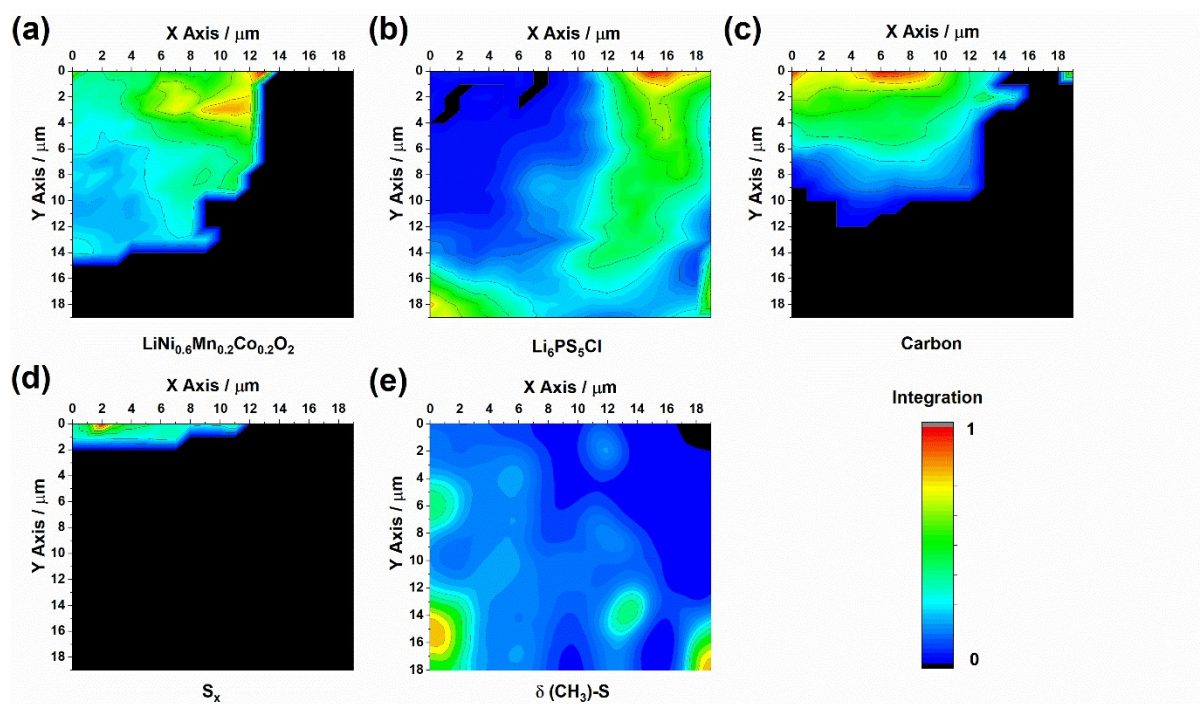


Figure S10. Raman mapping images of $\text{Li}_6\text{PS}_5\text{Cl}$ containing composite electrode after electrochemical test. (a) $\text{LiNi}_{0.6}\text{Mn}_{0.2}\text{Co}_{0.2}\text{O}_2$, (b) $\text{Li}_6\text{PS}_5\text{Cl}$, (c) carbon additive (VGCF), (d) S_x and (e) $\delta(\text{CH}_3)\text{-S}$.

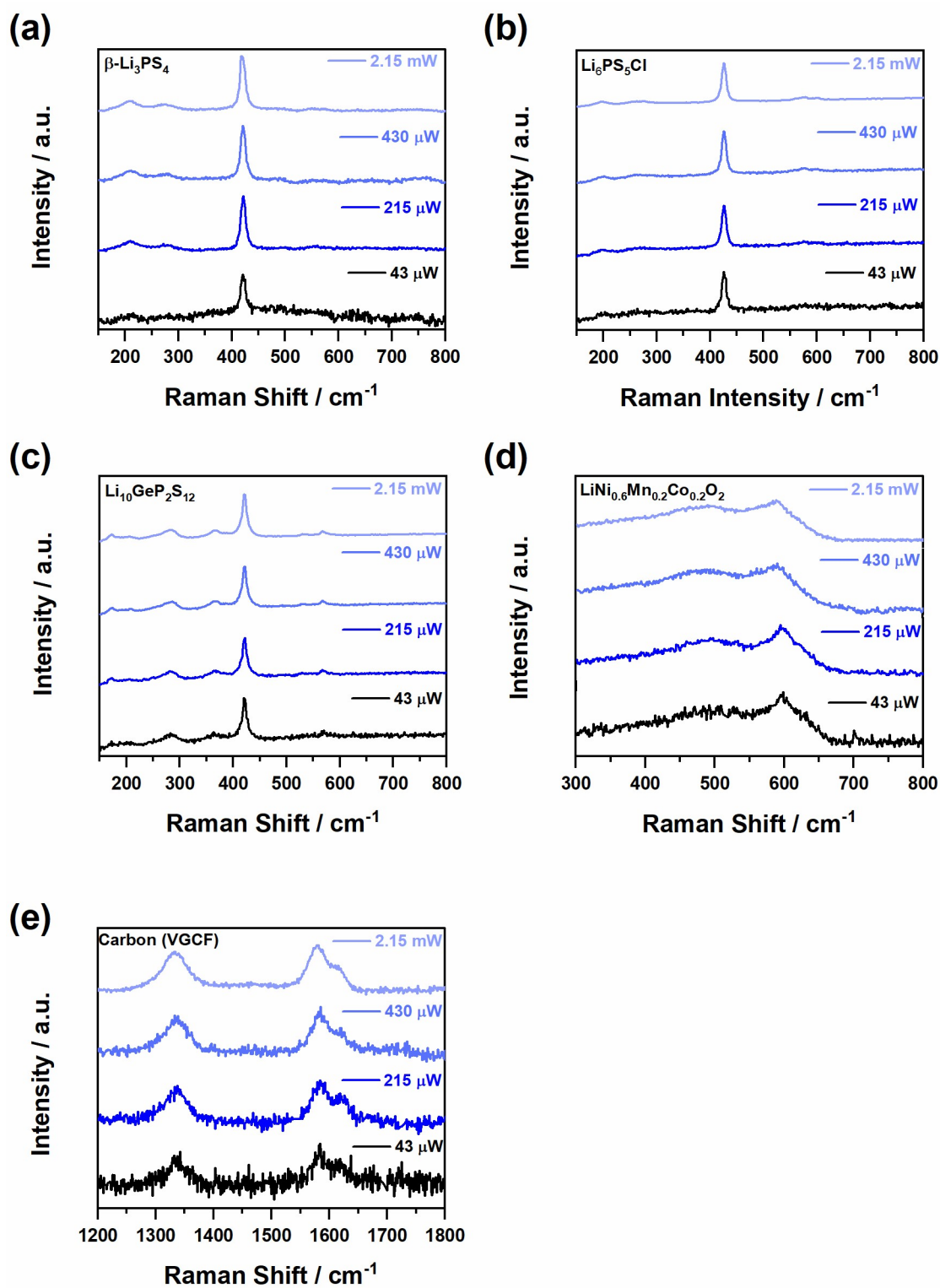


Figure S11. Raman spectra at various laser power for (a) $\beta\text{-Li}_3\text{PS}_4$, (b) $\text{Li}_6\text{PS}_5\text{Cl}$, (c) $\text{Li}_{10}\text{GeP}_2\text{S}_{12}$, (d) $\text{LiNi}_{0.6}\text{Mn}_{0.2}\text{Co}_{0.2}\text{O}_2$ and (e) Carbon (VGCF). Note for Raman mapping experiments, 43 μW laser power was used.